THE JOURNAL OF BIOLOGICAL CHEMISTRY VOL. 289, NO. 19, pp. 13323–13334, May 9, 2014

Modeling of Antigenomic Therapy of Mitochondrial Diseases by Mitochondrially Addressed RNA Targeting a Pathogenic Point Mutation in Mitochondrial DNA*[S]

Received for publication, October 21, 2013, and in revised form, March 20, 2014 Published, JBC Papers in Press, April 1, 2014, DOI 10.1074/jbc.M113.528968

Yann Tonin[‡1], Anne-Marie Heckel[‡], Mikhail Vysokikh[‡2], Ilya Dovydenko[‡§], Mariya Meschaninova[§], Agnès Rötig[¶], Arnold Munnich[¶], Alya Venyaminova[§], Ivan Tarassov[‡], and Nina Entelis[‡3]

From the [‡]UMR 7156 Génétique Moléculaire, Génomique, Microbiologie (GMGM), Strasbourg University-CNRS, Strasbourg 67084, France, the [§]Laboratory of RNA Chemistry, Institute of Chemical Biology and Fundamental Medicine SB RAS, Novosibirsk 630090, Russia, and the [¶]Université Paris Descartes-Sorbonne Paris Cité, INSERM U781, Hôpital Necker-Enfants Malades, Paris 75015, France

Background: Point mutations in mitochondrial genome cause severe clinical disorders.
Results: We designed recombinant RNA molecules imported into mitochondria of human cells, which are able to decrease the proportion of mitochondrial DNA molecules bearing a pathogenic point mutation.
Conclusion: Imported recombinant RNAs can function as anti-replicative agents in human mitochondria.
Significance: This is a new approach for therapy of mitochondrial diseases.

Defects in mitochondrial genome can cause a wide range of clinical disorders, mainly neuromuscular diseases. Presently, no efficient therapeutic treatment has been developed against this class of pathologies. Because most of deleterious mitochondrial mutations are heteroplasmic, meaning that wild type and mutated forms of mitochondrial DNA (mtDNA) coexist in the same cell, the shift in proportion between mutant and wild type molecules could restore mitochondrial functions. Recently, we developed mitochondrial RNA vectors that can be used to address anti-replicative oligoribonucleotides into human mitochondria and thus impact heteroplasmy level in cells bearing a large deletion in mtDNA. Here, we show that this strategy can be also applied to point mutations in mtDNA. We demonstrate that specifically designed RNA molecules containing structural determinants for mitochondrial import and 20-nucleotide sequence corresponding to the mutated region of mtDNA, are able to anneal selectively to the mutated mitochondrial genomes. After being imported into mitochondria of living human cells in culture, these RNA induced a decrease of the proportion of mtDNA molecules bearing a pathogenic point mutation in the mtDNA *ND5* gene.

RNA is increasingly used in therapeutic applications, including the agents of RNA interference, catalytically active RNA molecules, and RNA aptamers that bind proteins and other ligands (reviewed in Ref. 1). Here, we use RNA molecules imported into human mitochondria to suppress negative effects of mutations in mtDNA.[4] Involved in many metabolic pathways varying from cellular respiration to apoptosis, mitochondria are subcellular organelles essential for eukaryotic cells containing their proper genome, mtDNA. Human mtDNA is a closed circular double-stranded molecule of 16.5 kb able to replicate autonomously and encoding only 13 polypeptides, two ribosomal RNA (12 S and 16 S), and 22 tRNA, with the vast majority of mitochondrial proteins and several RNAs being encoded in the nucleus and imported from the cytoplasm. Multiple alterations may occur in the mitochondrial genome (deletions, duplications, and point mutations), resulting in severe impact on cellular respiration and therefore leading to many diseases, essentially muscular and neurodegenerative disorders. To date, >250 pathologic diseases were shown to be caused by defects in mtDNA (2). The majority of these mutations are heteroplasmic, meaning that mtDNA coexists in two forms, wild type and mutated, in the same cell. The occurrence and severity of pathologic effects depend on the heteroplasmy level, clinical symptoms appearing at the threshold of the order of 60 to 80%, depending on the mutation and the type of cells (3).

Various strategies have been proposed to address these pathologies, unfortunately, for the vast majority of cases, no efficient treatment is currently available. In some cases, defects may be rescued by targeting into mitochondria nuclear DNA-expressed counterparts of the affected molecules, an approach called allotopic strategy (4, 5). Allotopic expression of mtDNA-encoded polypeptides has been demonstrated in yeast, but in mammalian mitochondria, results are contradictory (reviewed

* The work was supported by CNRS, the University of Strasbourg, Association Française contre les Myopathies, Agence Nationale de la Recherche (ANR-06-MRAR-37-01; BLAN08-2-309449), Fondation pour la Recherche Médicale (DEQ20081214003), ARCUS/Suprachem Collaboration Program and LIA Collaboration Program (ARNmitocure). This work has also been published under the framework of the LABEX ANR-11-LABX-0057_MITOCROSS and is supported by the state managed by the French National Research Agency as part of the Investment for the Future program.
[S] This article contains supplemental movies.
[1] Supported by Fondation pour la Recherche Médicale and Association Française contre les Myopathies Ph.D. fellowships.
[2] Present address: Belozersky Institute of Physico-Chemical Biology, Moscow State University, Moscow 119992, Russia.
[3] To whom correspondence should be addressed: UMR 7156 Université de Strasbourg-CNRS, 21 Rue René Descartes, 67084 Strasbourg, France. Tel.: 33-3-68-85-14-81; Fax: 33-3-68-85-13-65; E-mail : n.entelis@unistra.fr.

[4] The abbreviations used are: mtDNA, mitochondrial DNA; TMRM, tetramethylrhodamine methyl ester.

in Ref. 6). We have exploited the RNA mitochondrial import pathway, which is the only known natural mechanism of nucleic acid delivery into mitochondria (reviewed in Ref. 7), to develop two successful models of allotopic rescue of an mtDNA mutation by targeting recombinant tRNA into mitochondria (8, 9).

Another strategy that might be termed as "anti-genomic," which consists of addressing into mitochondria endonucleases specifically eliminating mutated mtDNA, was also described (10, 11). Another approach, referred to as anti-replicative, aims to induce a shift in heteroplasmy level by targeting specifically the replication of mutant mtDNA, thus giving a propagative advantage to wild type genomes. This strategy has first been tested *in vitro* using peptide nucleic acids with high affinity to mutant mtDNA (12). It was demonstrated that peptide nucleic acid oligomers complementary to mutant mtDNA can specifically inhibit its replication *in vitro*; however, it remained non-applicable to living cells because of the impossibility of introducing peptide nucleic acid molecules into mitochondria *in vivo* (13). To overcome this obstacle, we proposed to use RNA mitochondrial import.

Analysis of the yeast $tRNA^{Lys}_{CUU}$ mitochondrial import mechanism demonstrated that binding to mitochondrial targeting protein factors and subsequent RNA translocation across mitochondrial membranes require formation of an alternative structure, different from a classic L-form tRNA model, characterized by bringing together the 3′-end and TΨC loop and forming the structure referred to as F-hairpin. Exploiting these data, we designed a short synthetic RNA comprising two domains of the yeast $tRNA^{Lys}_{CUU}$ alternative structure, D-arm and F-hairpin (referred to as FD RNA) (see Fig. 1), characterized by a high efficiency of mitochondrial targeting (14). These molecules, fused to oligonucleotide stretches complementary to the mtDNA-mutated region, were able to shift a heteroplasmy level in cells containing a large deletion in mtDNA, providing the first validation of the anti-replicative approach *in vivo* (15).

Here, we show that this approach is not limited to large rearrangements in mtDNA but can be applied to point mutations. We provide a protocol to design an oligonucleotide able to anneal to mtDNA bearing a point mutation but not to wild type mtDNA and an original assay to test the specificity of hybridization *in vitro*. A series of recombinant molecules, including RNA-DNA chimera, have been tested for mitochondrial import in human cultured cells and their ability to induce a shift of the heteroplasmy level. We demonstrate that RNA molecules containing mitochondrial targeting determinants and a 20-nucleotide sequence corresponding to the mutated region of mtDNA are able to selectively target mutated mitochondrial genomes. After being imported into mitochondria of cultured *trans*-mitochondrial human cells bearing a pathogenic point mutation in *ND5* gene, these RNA significantly decreased the proportion of mutated mtDNA molecules.

EXPERIMENTAL PROCEDURES

Recombinant RNA Modeling and Synthesis—To predict secondary structures of recombinant RNA and estimate their free energy (dG), the Mfold (16), IDT Sci-Tools OligoAnalyser (version 3.1), and ViennaRNA platforms were used. To estimate melting temperatures for DNA-DNA and RNA-DNA duplexes, we used IDT Sci-Tools OligoAnalyser software (version 3.1) (17).

The recombinant RNAs were obtained by T7 transcription using the T7 RiboMAX Express Large Scale RNA Production System (Promega) on the corresponding PCR products and were gel-purified. For PCR, the following oligonucleotides containing a T7 promoter (*underlined*) were used: *FD16L* (5′-TAA TAC GAC TCA CTA TAG CGC AAT CGG TAG CGC ACT CCA AAG GCC ACA TGA GCC CCC TAC AGG GCT C-3′); *FD16H* (5′-TAA TAC GAC TCA CTA TAG CGC AAT CGG TAG CGC ATG TGG CCT TTG GAG TGA GCC CCC TAC AGG GCT C-3′); *FD20L* (5′-TAA TAC GAC TCA CTA TAG CGC AAT CGG TAG CGC ACT CCA AAG GCC ACA TCA TCG AGC CCC CTA CAG GGC TC-3′); *FD20H* (5′-TAA TAC GAC TCA CTA TAG CGC AAT CGG TAG CGC GAT GAT GTG GCC TTT GGA GTG AGC CCC CTA CAG GGC TC-3′); *FD25L* (5′-TAA TAC GAC TCA CTA TAG CGC AAT CGG TAG CGC GTT TCT ACT CCA AAG GCC ACA TCA TGA GCC CCC TAC AGG GCT C-3′); *FD25H* (5′-TAA TAC GAC TCA CTA TAG CGC AAT CGG TAG CGC ATG ATG TGG CCT TTG GAG TAG AAA CGA GCC CCC TAC AGG GCT C-3′) with primers T7 (5′-GGG ATC CAT AAT ACG ACT CAC TAT A-3′) and FD-rev (5′-AAG AGC CCT GTA GGG-3′).

To test recombinant RNA annealing to target mtDNA, fragments of wild type and mutant mtDNA were amplified using primers hmtGluRT (5′-GTT CTT GTA GTT GAA ATA C-3′) and CRC-F (5′-CAT ACC TCT CAC TTC AAC CTC C-3′), separated on 1% agarose gel, blotted to Hybond-N membrane, and hybridized with ^{32}P-labeled recombinant RNAs in 1× PBS at 37 °C. After PhosphorImager quantification (Typhoon Trio, GE Healthcare), the hybridization signals were normalized to amounts of corresponding mtDNA fragments calculated after ethidium bromide staining of the agarose gel (before transfer to Hybond membrane) by densitometry using G-Box and GeneTools analysis software. Thereafter, hybridization specificity was calculated for each RNA as one minus ratio between normalized signals for wild type and mutated DNA fragments. Thus, for recombinant RNA annealed only to mutant DNA fragment, the hybridization specificity value reached 1, and for RNA annealed equally to mutant and wild type fragments, this value was close to 0. At least three independent experiments were performed for each RNA.

Chimeric Oligonucleotide Synthesis—Chimeric oligonucleotides D20L DNA and D20H DNA were synthesized on an automatic ASM-800 RNA/DNA synthesizer (Biosset) at 0.4-μmol scale using solid phase phosphoramidite synthesis protocols (18) optimized for this instrument. The DNA and 2′-*O*-TBDMS (*tert*-butyldimethylsilyl)-protected RNA phosphoramidites and appropriate supports were purchased from Glen Research. A 5-ethylthio-*H*-tetrazole has been used as activator with 5- and 10-min coupling steps, respectively. After standard deprotection, oligonucleotides were purified by 12% polyacrylamide/8 M urea gel and characterized by MALDI-TOF mass spectrometry (Autoflex III, Bruker Daltonics).

Synthesis of Fluorescently Labeled RNA Transcript—Alexa Fluor 488-5 UTP (Molecular Probes) was incorporated into RNA during 2-h T7 transcription by T7 RNA polymerase (Promega). A reaction mixture of 20 μl total volume contained 0.5 μg of DNA template, 80 units of T7-RNA polymerase (two additions of 40 units each), 0.5 mM ATP, 0.5 mM CTP, 0.5 mM GTP, 0.37 mM UTP, 0.125 mM Alexa Fluor 488-5-UTP, 10 mM DTT, and 40 units of RNaseOUT (Invitrogen). T7 transcript was purified by PAGE. To check the incorporation of the label in purified transcript, we compared the dye absorbance at 492 nm with the absorbance at 260 nm using NanoDrop ND1000 Microarray software (version 3.5.2). The efficiency of labeling obtained was approximately two labeled uridines per one RNA molecule.

RNA FD20H, used for the microscopy, contains 13 uridine residues (see Fig. 2): one at the end of F-stem region, three in the loops, and nine in the anti-replicative part of the molecule, which is not responsible for the mitochondrial import efficiency. Therefore, the labeling should not significantly alter the secondary structure and mitochondrial import of the RNA molecule.

Transient Transfection of Cybrid Cells—*Trans*-mitochondrial cybrid cell lines obtained by fusion of fibroblast-derived cytoplast from patient and a 143B rho^0 cell line (19) were kindly provided by M. Zeviani (National Neurological Institute "Carlo Besta," Milan, Italy).

Primary skin fibroblasts were from patient 1: a boy born to non-consanguineous healthy parents. He was completely normal until 13 years of age when he developed dystonia of the left hand that worsened progressively. A brain MRI at 14 years of age revealed hypersignal of basal ganglia and abnormalities of brain system consistent with the diagnosis of Leigh syndrome. Two years later, he had tonicoclonic seizures with nystagmus and dysarthria. Stroke-like pattern was detected by brain MRI. Measurement of respiratory chain activities detected an isolated complex I deficiency related to a mitochondrial DNA mutation in the *ND5* gene (A13514G). Fibroblasts were characterized by a 30% heteroplasmy level. Cells were cultivated at 37 °C and 5% CO_2 in DMEM (Sigma) containing 4.5 g/liter of glucose supplemented with fetal calf serum (Invitrogen), penicillin/streptomycin, uridine (50 mg/liter), and fungizone (2.50 mg/liter) (Invitrogen).

Transient transfection of cells with RNA and chimeric molecules was performed as described in Refs. 20 and 21 with some modifications: for 2 cm^2 well of 80% confluent cells, we used 0.25 μg of RNA and 1 μl of Lipofectamine 2000 in OptiMEM medium (Invitrogen). OptiMEM was changed to a standard DMEM medium 8 h after transfection. In these conditions, ~80% of fibroblasts and 95% of cybrid cells were transfected with RNA (evaluated by fluorescent microscopy and by flow cytometry using CyFlow FACS 24 h post transfection). We also compared Northern hybridization signals obtained on total cellular RNA and on the known amounts of T7 transcripts loaded on the same gel. We could estimate that ~15% of RNA added to cybrid cells and 20% RNA for fibroblasts were internalized and can be detected in full-size form 24 h post transfection (data not shown). Transfection procedure did not lead to detectable decrease of viability of the cells or to a significant change of the overall mtDNA amount verified by real-time quantitative PCR as described (15).

RNA Stability and Mitochondrial Import in Vivo—Mitochondria were isolated from the cybrid cells as described previously (22, 23) and treated with digitonin to generate mitoplasts (mitochondria devoid of the outer membrane) and RNase A to get rid of non-specifically attached RNA. This treatment allows us to obtain mitochondria free of cytosolic RNA contamination, which was tested using a probe for cytosolic 5.8 S rRNA usually strongly attached to the outer mitochondrial membrane. Total and mitochondrial RNA was isolated with TRIzol reagent (Invitrogen). Stability and mitochondrial import of recombinant molecules were analyzed by Northern hybridization of total and mitochondrial RNA with ^{32}P-labeled oligonucleotide probes followed by PhosphorImager quantification (Typhoon-Trio, GE Healthcare).

The probes used were as follows: "D-loop" probe-specific for recombinant molecules (see Fig. 1), 5′-GAG TCA TAC GCG CTA CCG ATT GCG CCA ACA AGG C-3′, hybridization temperature of 50 °C; cytosolic 5.8S rRNA probe, 5′-GGC CGC AAG TGC GTT CGA AG-3′, hybridization temperature of 50 °C; probe against the mitochondrial tRNA^{Val}, 5′-GAA CCT CTG ACT GTA AAG-3′, hybridization temperature of 45 °C; probe against the nuclear snRNA U3, 5′-CGC TAC CTC TCT TCC TCG TGG-3′, hybridization temperature of 50 °C. To compare the stability of different recombinant RNA, the relative concentration of each RNA in various time periods after transfection was calculated as a ratio between the D-loop probe signal and the signal for cytosolic 5.8 S rRNA.

The relative amount of each imported RNA inside the mitochondria was estimated as a ratio between the signal obtained after hybridization with the D-loop probe and the signal with a probe against the mitochondrial tRNA^{Val} in the same RNA preparation. To compare import efficiencies of different RNA molecules, the total level of each RNA molecule in transfected cells was taken into account and normalized as described previously (22). At least three independent experiments were performed for each RNA.

Confocal Microscopy—Cybrids cells cultivated in 2-cm^2 chamber slides (Lab-Tek) were transfected with Alexa Fluor 488-5-UTP-labeled RNA. At different time periods after transfections, living cells were stained with 5 μM tetramethylrhodamine methyl ester (TMRM) for 15 min at 37 °C, washed, and imaged in DMEM without red phenol. The LSM 700 confocal microscope (Zeiss) was used in conjunction with Zen imaging software, and images were acquired with a Zeiss 63×/1.40 oil immersion objective with a resolution of 1024 × 1024. The excitation/emission laser wavelengths were 488 nm (green channel) and 555 nm (red channel). Images were analyzed using ImageJ software (24) and JACoP plugin (25). Co-localization analyses were performed on multiple cells and optical sections. Pearson's and Manders' coefficients were estimated (26, 27). Pearson's correlation coefficient provides a measure of correlation between the intensities of each channel in each pixel. The overlap coefficients according to Manders indicate an actual overlap of the signals and represent the true degree of co-localization. In control experiments, cells were transfected with

Alexa Fluor 488-5-UTP-labeled RNA, which is not imported into mitochondria (28).

mtDNA Heteroplasmy Level Analysis—To isolate total DNA from transfected cells, 1 cm^2 of cells were solubilized in 0.5 ml of buffer containing 10 mM Tris-HCl, pH 7.5, 10 mM NaCl, 25 mM Na-EDTA, and 1% SDS, then 10 μl of proteinase K solution (20 mg/ml) was added, and the mixture was incubated for 2 h at 50 °C; 50 μl of 5 M NaCl was added, the DNA was precipitated with isopropyl alcohol and used for PCR amplification. Heteroplasmy level was analyzed by restriction fragment length polymorphism on a 125-bp PCR fragment encompassing nucleotides 13430 to 13555 of mtDNA obtained with primers CRC-F 5′-CAT ACC TCT CAC TTC AAC CTC C-3′ and CRC-R 5′-AGG CGT TTG TGT ATG ATA TGT TTG C-3′ (19). The A13514G mutation creates a HaeIII-specific cleavage site, giving two fragments of 80 and 45 bp. The HaeIII-digested fragments were separated on a 10% PAGE and stained with ethidium bromide. The proportion of mutant *versus* total mtDNA was calculated by densitometry using G-Box and GeneTools analysis software (Syngene). At least four independent transfections were performed with each recombinant RNA. Each DNA sample was analyzed twice by PCR amplification followed by at least three gel separation and quantification experiments.

The digestion control was performed for each reaction. For this, a 600-bp PCR fragment encompassing nucleotides 1216 to 1813 of mtDNA obtained with the primers CRS-F (5′-CGA TAA ACC CCG ATC AAC CTC-3′) and CRS-R (5′- GGT TAT AAT TTT TCA TCT TTC CC-3′) was cleaved by HaeIII to 350- and 250-bp fragments in the same tube as 125-bp PCR fragment containing the A13514G mutation site.

Mitochondria Quantification—2-cm^2 wells of 80% confluent cybrid cells and control wild type 143B cells, transfected with FD20H RNA, were stained with 5 μM TMRM and 200 nM MitoTracker® Green during 15 min in culture medium. The intensity of fluorescence was directly measured in a culture plate in DMEM without red phenol by VICTOR™ X3 multilabel plate reader (PerkinElmer Life Science) at 485 nm (green channel) and 555 nm (red channel) in triplicate for each sample. After fluorescence measurement, cells were detached and quantified by flow cytometry using CyFlow FACS and FloMax software (Partec). Activity of complex I was measured using a MitoSciences® kit (Abcam).

Statistical Analyses—Pairwise comparisons were performed using two-tailed Student's *t* test and Excel software (Microsoft). Data are expressed as means ± S.D.

RESULTS

Design of Anti-replicative RNA Molecules—As it was reported previously, the helix-loop domains of FD RNA can serve as signals for RNA mitochondrial import, and this molecule can be used as a vector to deliver various sequences into the organelles (15). Recently, we also demonstrated that only one D-arm structure can be sufficient for targeting of recombinant molecule to mitochondria in living cells (28, 29).

To apply the anti-genomic strategy to point mutations, we used as a model the A13514G mutation inducing amino acid replacement D393G in the *ND5* gene of human mtDNA, which encodes one of the membrane domain subunits of the respiratory complex I (30). This mutation was initially found in two unrelated patients with MELAS (mitochondrial encephalopathy, lactic acidosis, and stroke-like episodes)-like syndrome (19). To target the mutant mitochondrial genome, a series of RNA molecules were constructed, bearing sequences complementary to a mutated region of *ND5* gene inserted between two helix-loop domains of a short artificial FD RNA (Fig. 1).

First, we analyzed the secondary structure predictions for FD RNA molecules bearing insertions of 16, 20, and 25 nucleotides corresponding to a fragment of the *ND5* gene, referred to as FD16L, FD16H, FD20L, FD20H, FD25L, and FD25H; R for sequence of H-strand and S for L-strand of mtDNA. For each sequence, a series of insertions bearing nucleotide G or C corresponding to the mutation A13514G (for either H- or L-strand) in various positions (Fig. 1) were analyzed by several types of software (see "Experimental Procedures") with similar results. Only molecules with a low probability of alternative folding were retained for further studies (Fig. 1). To check the ability of the selected versions for a specific annealing with mutated, but not wild type mtDNA, labeled recombinant RNAs were hybridized under physiological conditions with PCR-amplified mtDNA fragments either containing the mutation or not (Fig. 2). Versions FD25L and FD25H were not able to discriminate between mutant and wild type mtDNA; the shorter RNA molecule FD20H (but not FD20L) demonstrated specific annealing with the A13514G bearing mtDNA but not wild type. Annealing of molecules FD16H and FD16L was rather specific for mutant mtDNA; however, the efficiency of their hybridization at 37 °C was reproducibly lower when compared with FD20H. We also tested chimeric molecules, containing a stem-loop RNA import determinant and DNA inserts corresponding to FD20H and FD20L sequences, referred to as D20H-DNA and D20L-DNA (Fig. 2). Chimeric RNA-DNA molecule D20L-DNA demonstrated a higher ability to discriminate between mutant and wild type mtDNA when compared with FD20L. Thus, the recombinant molecules with 20 nucleotide insertions (FD20L, FD20H, D20L-DNA, and D20H-DNA) have been selected for the further analysis.

Mitochondrial Import of Recombinant RNA—To study the localization of recombinant RNA molecules in cultured human cells, an approach was developed consisting in cell transfection with Alexa Fluor 488-labeled RNA FD20H and its subsequent co-localization with the mitochondrial network by means of fluorescent confocal microscopy (Fig. 3). RNA molecules (green fluorescence) were detectable in cells in 24 h after transfection (day 1) as *green dots*, most probably representing the RNA-Lipofectamine complexes, with only slight co-localization with the mitochondria (red fluorescence). In 2–4 days after transfection, the distribution of the green label changed drastically, the amount of dots was reduced, and RNA molecules were now mostly dispersed within the cell, displaying clear partial co-localization with the mitochondrial network (Fig. 3*B* and supplemental movies). To perform quantitative co-localization analysis of confocal microscopy images, we estimated the values of Pearson's correlation coefficient and Manders' overlap coefficients M1 and M2 (26). For control RNA that is not imported into mitochondria (28), all of the coefficient values were very low (Fig. 3*A*), thus excluding the coincidental overlap

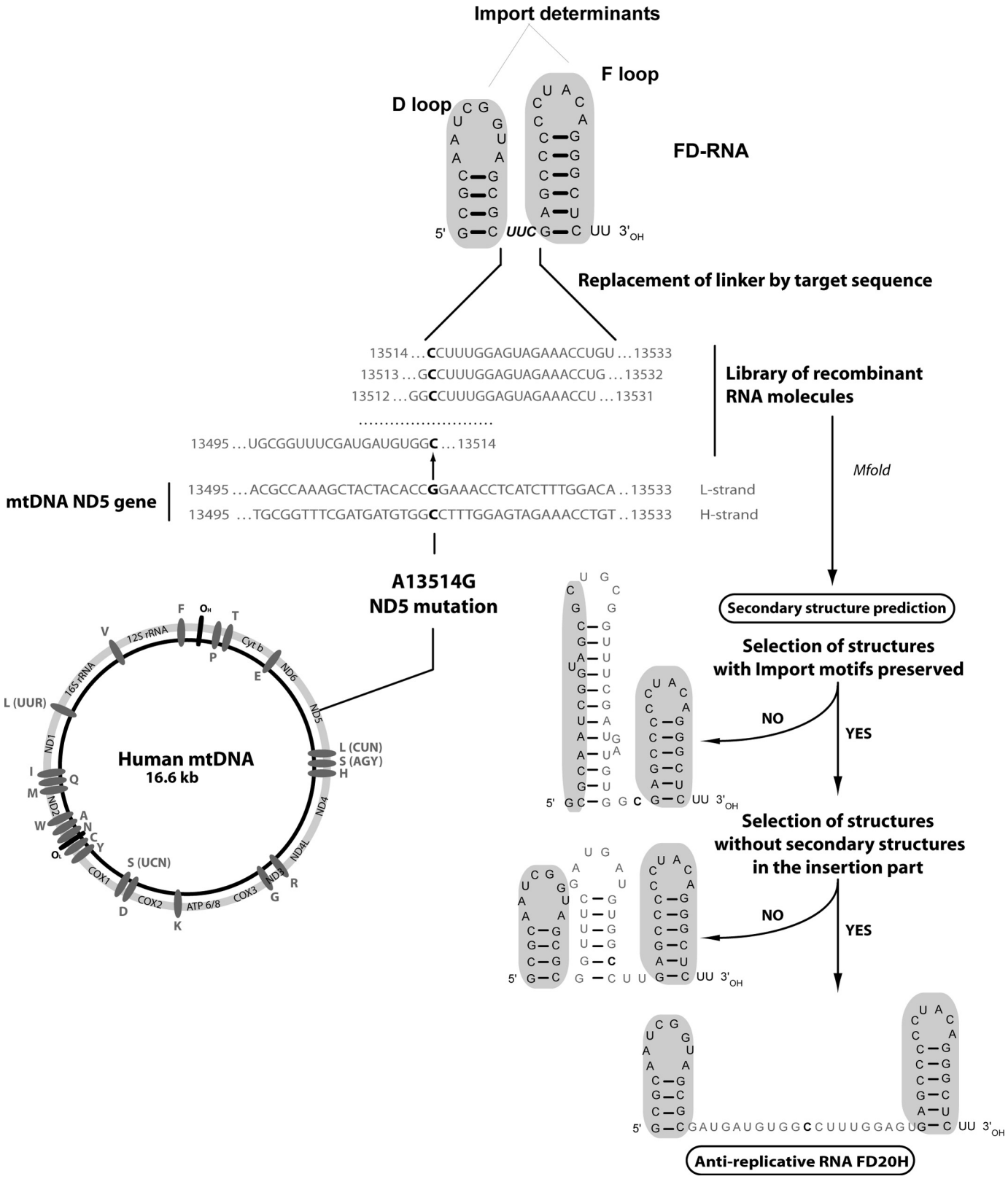

FIGURE 1. **Design of anti-replicative RNAs targeting A13514G mutation in human mtDNA.** Human mtDNA genetic map and sequence of the mutated region of *ND5* gene are presented, A13514G mutation is shown in *boldface type*; the FD-RNA stem-loop import determinants are colored *gray*. Design of recombinant RNA FD20H containing 20-mer corresponding to the H-strand of mtDNA is shown (see text for details).

of green and red signals. For FD20H RNA, the M1 values indicated that in 2 days post transfection, ~50% of green fluorescence (RNA) has been co-localized with red fluorescence (mitochondria), and this level did not significantly change between 2 and 4 days post transfection. M2 values representing the percentage of the red fluorescence (mitochondria) overlap-

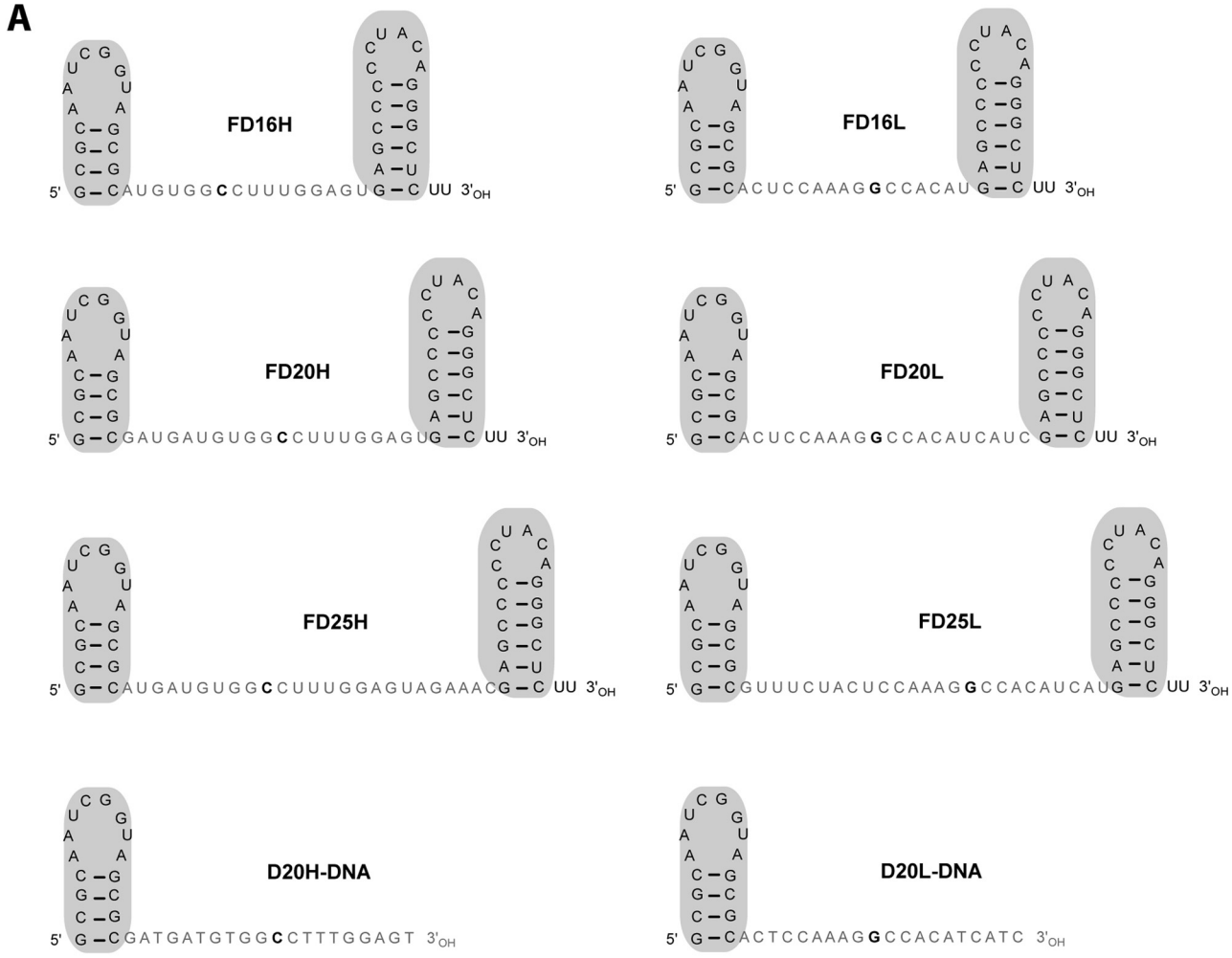

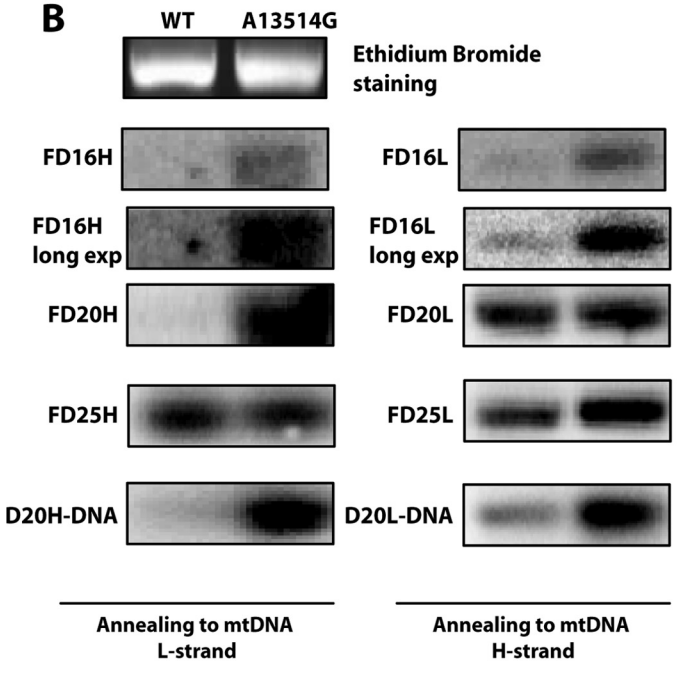

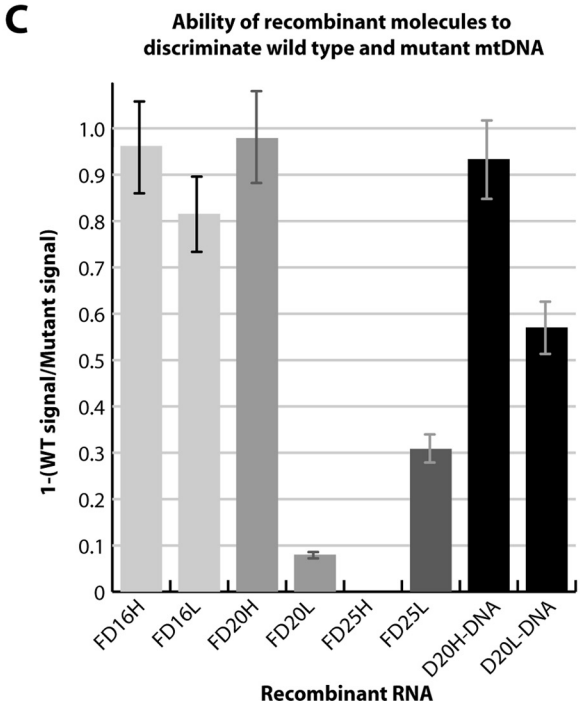

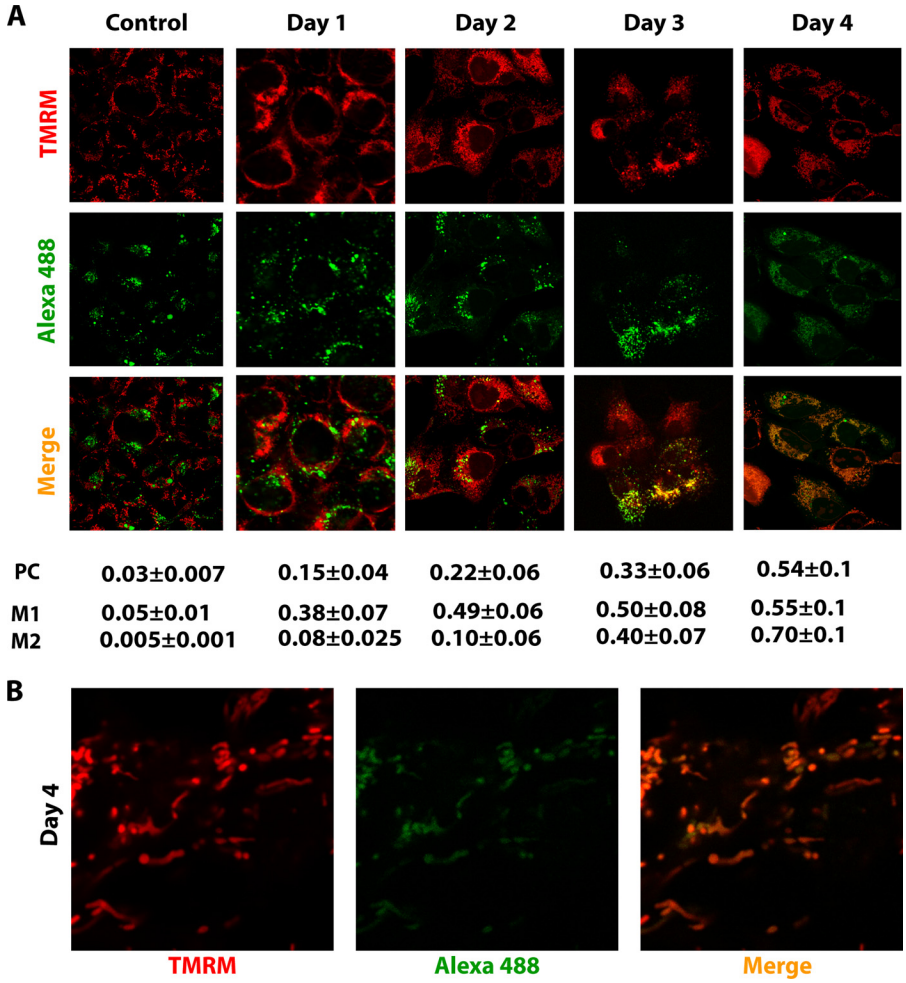

FIGURE 3. **Confocal microscopy of human cells transfected with fluorescently labeled RNA.** *A*, confocal microscopy of 143B cells transfected with Alexa Fluor 488-labeled FD20H RNA (*green*) at various time periods after transfection (as indicated *above* the panels). Control, cells transfected with Alexa Fluor 488-5-UTP-labeled RNA, which is not imported into mitochondria, 3 days post transfection. *TMRM*, visualization of mitochondrial network by red staining. *Below* the panels, shown is quantification of RNA co-localization with mitochondria, estimated for multiple cells and 6–10 optical sections in two independent experiments. *PC*, Pearson's correlation coefficient; *M1* and *M2*, Manders' overlap coefficients, representing the percentage of green fluorescence co-localized with red fluorescence (for M1) and the percentage of red fluorescence co-localization with green fluorescence (for M2). *B*, magnification of the image corresponding to day 4 post transfection. A three-dimensional reconstruction of the confocal microscopy image by ImageJ software is presented in the supplemental movies.

ping with the green fluorescence (RNA) indicate that only 10% of mitochondria contained RNA in 2 days post transfection. This proportion has been increased in 3 and 4 days up to 70%, probably due to the mitochondrial dynamic events, fusion and fission, resulting in more homogenous RNA distribution. These data clearly indicate on mitochondrial targeting of FD20H RNA in living human cells.

To measure recombinant RNA stability in cultured cells and the efficiency of their import into the mitochondrial matrix, cybrid cells were transfected with *in vitro*-synthesized recombinant RNAs and chimeric molecules. Their degradation rate in transfected cells was evaluated by Northern hybridization of total cellular RNA at different time points spanning a 6-day period after transfection (Fig. 4*A*). Recombinant molecules were detectable in cybrid cells at least 6 days after transfection. The chimeric version D20L DNA revealed to be more stable than FD20L and FD20H. Such result suggests that the "insertion" part, lacking strong secondary structures, gives a prominent impact on the degradation of recombinant molecules. Thus, recombinant molecules in which RNA insertions were replaced by DNA sequences demonstrated improved stability in the living cells.

Because the microscopy data can give only a rough indication on the mitochondrial import of RNA molecules, we performed

FIGURE 2. **Ability of recombinant molecules to discriminate wild type and mutant mtDNA.** *A*, predicted secondary structures of anti-replicative molecules. Stem-loop import determinants are shown in *gray*. D20H DNA and D20L DNA, chemically synthesized chimeric molecules, RNA insertion has been replaced by DNA. *B*, Southern hybridization of WT or mutant (A13514G) mtDNA fragments with labeled recombinant RNAs (indicated at the *left*) under physiological conditions. *Long exp.*, radiogram after longer exposition for FD16H and FD16L. The specific radioactivity of all of the RNA probes was comparable. *C*, graphical representation of hybridization specificity of different recombinant molecules (indicated *below* the graphs). The hybridization specificity was calculated for each RNA as 1 − (ratio between hybridization signals for wild type and mutated DNA fragments). Thus, for recombinant RNA annealed only to the mutant DNA fragment, the hybridization specificity value reached 1, and for RNA annealed equally to mutant and wild type fragments, this value was close to 0. Data are ± S.D. calculated from three independent experiments.

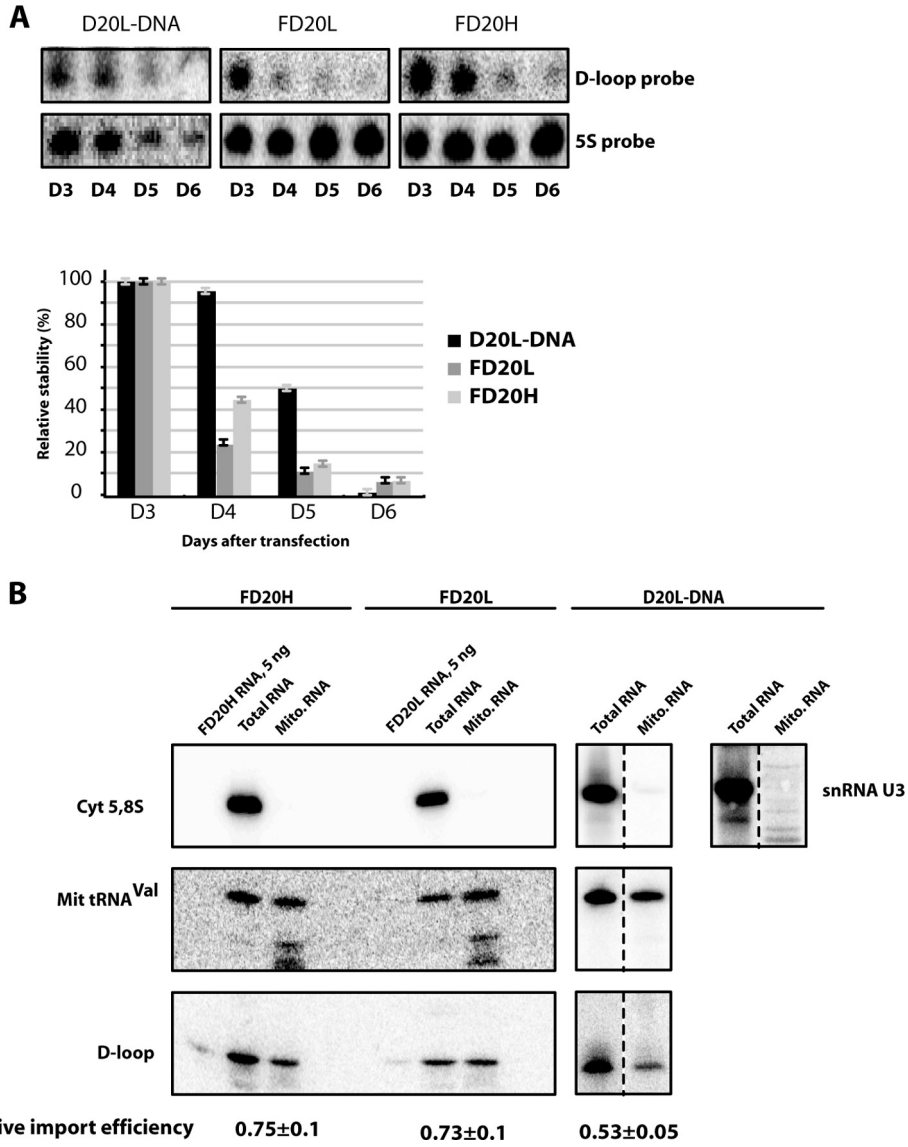

FIGURE 4. **Anti-replicative RNA stability and mitochondrial import in transiently transfected cybrid cells.** *A*, an example of Northern hybridization of total RNA isolated in 3–6 days after cell transfection (as indicated *below*) with various recombinant molecules (indicated *above* the panels). Probes used for hybridization: D-loop, specific for all recombinant molecules used for transfection; *5S*, against 5 S rRNA to quantify the level of recombinant RNA in the cells. Time dependence of RNA decay is shown below (means ± S.D. calculated from at least four independent experiments). *B*, mitochondrial import of recombinant molecules in transiently transfected cybrid cells. Northern hybridizations of RNA extracted from cells (*Total RNA*) or purified mitoplasts (*Mito RNA*) 48 h after transfection. *Above*, RNAs used for transfection are indicated. On the *left*, hybridization probes: D-loop, specific for recombinant molecules used for the transfection; *Cyt 5.8S*, against 5.8 S rRNA to check the absence of cytosolic RNA in mitochondrial samples; *snRNA U3*, demonstrating that the mitoplast fraction was not contaminated by the small nuclear RNAs; *Mit tRNA*^{Val}, to normalize the level of recombinant RNA to amount of loaded material. Import efficiency was estimated as a ratio of mitochondrial to total signal for the D-loop probe after normalization of the both signals to those for mitochondrial tRNA^{Val} probe.

Northern blot hybridization experiments. For this, cells were transfected with purified recombinant molecules. The mitochondrial import was analyzed by hybridization of the whole cell RNA and RNA isolated from purified and RNase-treated mitoplasts (mitochondria where the outer membrane was removed by digitonin) as described previously (15, 22, 29). The absence of signal in the mitochondrial RNA preparation after hybridization with the probe against the cytoplasmic 5.8 S rRNA indicates that the treatment of mitochondria with ribonuclease and digitonin removed all contamination by cytoplasmic RNA (Fig. 4*B*). Hybridization signals obtained with the D-loop probe specific for all of the recombinant molecules were normalized to the amounts of loaded RNA, estimated by hybridization with a probe to a mitochondrial transcript (*mito tRNA*^{Val}). The data show that the import efficiencies of RNA molecules FD20H and FD20L were close to each other; import of the chimeric molecule D20L-DNA was only slightly decreased (Fig. 4*B*).

Imported RNA Can Shift Point Mutation Heteroplasmy Level in Cybrid Cells—Trans-mitochondrial cybrid cell line containing a patient's mitochondria with 35% of mtDNA molecules bearing an A13514G mutation (referred thereafter as *ND5* mutation) were transfected with *in vitro* synthesized recombinant RNA and chimeric RNA-DNA molecules. Heteroplasmy levels (percentage of mutant *ND5* mtDNA to all mtDNA molecules) were measured at different time points after transfection by restriction fragment length polymorphism analysis of

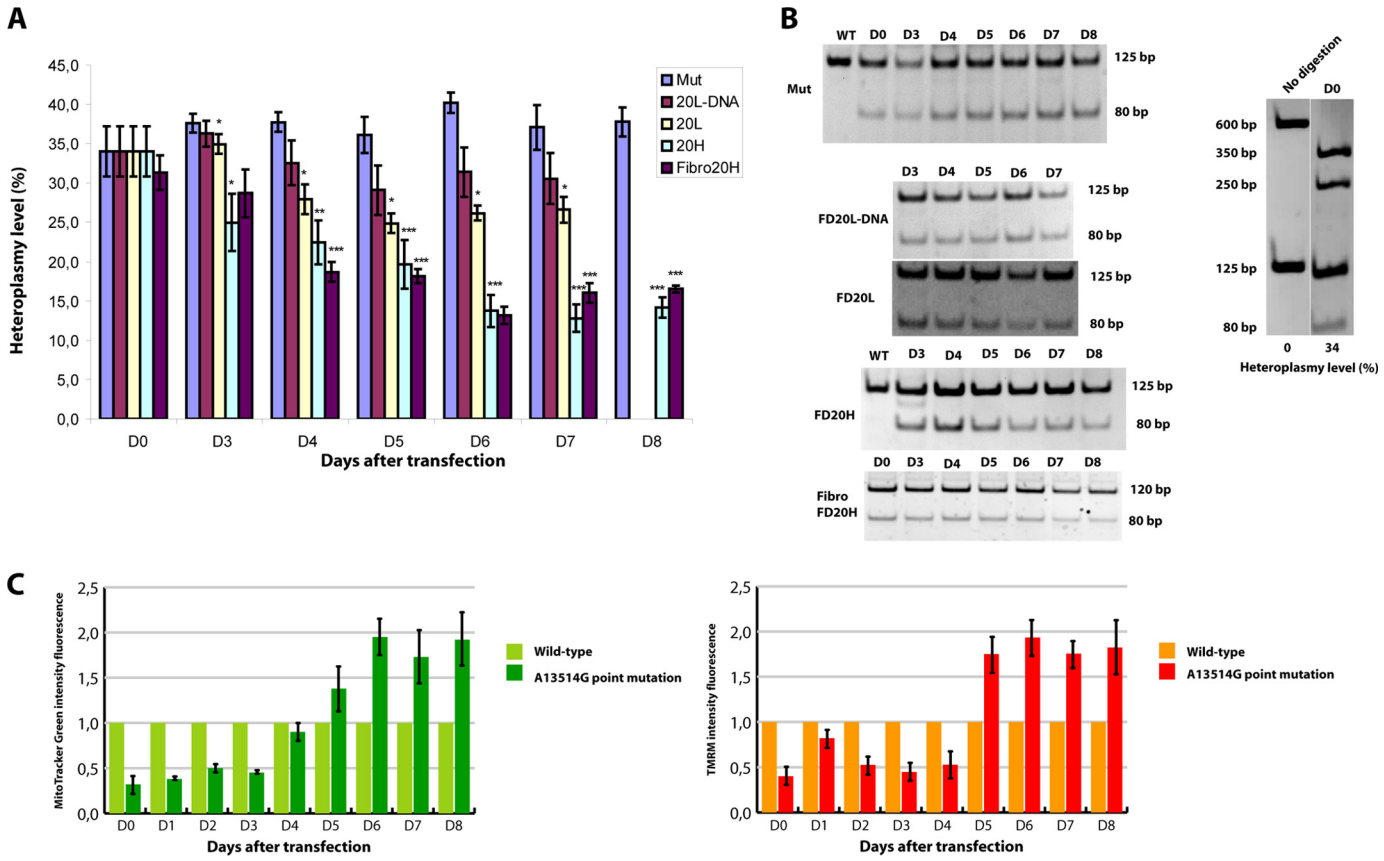

FIGURE 5. **The effect of recombinant RNA on heteroplasmy level in transfected cybrid cells.** *A*, time dependence of A13514G mutation heteroplasmy level (axis Y) followed during 7–8 days. *D0–D8*, days after transfection of cells with different recombinant molecules. *Mut*, mock-transfected cybrid A13514G cells; *WT*, mock-transfected 143B cells; FD20L, FD20H, or FD20L-DNA, cybrid cells transfected with corresponding recombinant molecule; *Fibro 20H*, primary fibroblasts transfected with FD20H RNA. Data are expressed as mean ± S.D. for 3–5 independent experiments. Shown is an unpaired *t* test between values for mutant and transfected cells; *, $p < 0.02$; **, $p < 0.003$; ***, $p < 0.0009$. *B*, an example of restriction fragment length polymorphism (*RFLP*) analysis for DNA samples isolated in 3–8 days (as indicated above) after cybrid cell transfection with recombinant molecules indicated at the left. Digestion control was performed for each reaction, as shown at the *right panel*. For this, 600-bp PCR fragment of mtDNA was cleaved by HaeIII to 350- and 250-bp fragments in the same tube as 125-bp PCR fragment spanning A13514G mutation site. The A13514G mutation creates an HaeIII-specific cleavage site, giving the fragment of 80 bp. Fragment size is indicated for each panel. *C*, evaluation of total and energised mitochondria content in 143B (wild type) and cybrid cells (A13514G) transfected with RNA FD20H during 8 days after cell transfection. MitoTracker Green (*left panel*) and TMRM (*right panel*) fluorescence normalized to the number of cells; values of wild type cells were taken as 1.

PCR-amplified mtDNA fragment (Fig. 5, *A* and *B*). We observed a reproducible decrease of the proportion of mutant mtDNA in cells transfected by recombinant RNA containing FD20H inserts. The heteroplasmy shift became visible 3 days after transfection, and then the heteroplasmy continued to decrease and reached the stable level of 13 ± 2% in 6 days post transfection. To affirm these data, we performed transfection of patient's fibroblasts, harboring the A13514G mutation, with FD20H RNA (Fig. 5, *A* and *B*). This completely independent experiment on primary human cells gave the same result of heteroplasmy shift, as obtained on the cybrid cells model.

Remarkably, in cells transfected with FD20H RNA, the decrease of mutant mtDNA correlated to increased amount of mitochondria per cell measured as MitoTracker Green fluorescence (Fig. 5*C*). Moreover, the same increase of the fluorescence was detected by TMRM dye that is readily sequestered by active mitochondria, indicating on a fully energized state of mitochondrial membranes (31).

In parallel experiments, mock-transfected cybrid cells demonstrated no heteroplasmy shift (Fig. 5, *A* and *B*). Cell transfection with FD20L RNA led to a very small heteroplasmy decrease, reaching the level of 27 ± 5% in 7 days (Fig. 5*A*). Different effects of FD20H and FD20L RNA molecules are in perfect correlation with the more specific hybridization of FD20H RNA with mutant mtDNA (Fig. 2). Surprisingly, chimeric molecule D20L DNA, characterized by a rather specific hybridization with mutant mtDNA *in vitro*, high stability in cells, and efficient import into mitochondria, was not able to influence the heteroplasmy level. Our data show that mitochondrially imported RNA (but not DNA) molecules can function as anti-genomic agents in human cells, affecting the amount of mitochondrial genomes bearing a point mutation.

DISCUSSION

Specific Annealing of RNA to mtDNA Bearing a Point Mutation—The anti-replicative approach aiming to shift heteroplasmy levels in mtDNA below the pathogenic threshold has been recently applied to cells containing a large 7-kb deletion in mtDNA (15). In this case, a new sequence generated at the fusion of the deletion boundaries has been inserted into RNA vector molecules, and specific annealing only with the mutant but not with wild type mtDNA was demonstrated for recombi-

TABLE 1
Melting temperature predictions for hybrids between recombinant RNAs and mutated or WT mtDNA regions

RNA	Insert (bp)	T_m for mutated DNA	T_m for WT DNA[a]	ΔT_m
FD16L	16	48.4 °C	40.2 °C	8.2 °C
FD16H	16	48.4 °C	35.0 °C	13.4 °C
FD20L	20	54.9 °C	49.3 °C	5.6 °C
FD20H	20	52.8 °C	42.9 °C	9.9 °C
FD25L	25	59.0 °C	54.9 °C	4.1 °C
FD25H	25	59.0 °C	52.2 °C	6.8 °C

[a] Shown are values predicted by IDT Sci-Tools OligoAnalyser software (version 3.1) for mismatch containing DNA-DNA hybrids. ΔT_m, predicted decrease of T_m for wild type mtDNA compared with mutated mtDNA.

nant RNA molecules. In the present study, we investigated whether this strategy can be extended to point mutations in the mitochondrial genome. The first question we addressed was as follows: could a recombinant RNA importable into human mitochondria anneal in a specific way with only the mutant mtDNA containing a point mutation but not with wild type?

Using Southern hybridization under conditions designed to approximate the intracellular ionic environment, we demonstrated that the sequence of 20 nucleotides corresponding to H-strand of the mutated (A13514G) region of mtDNA (FD20H) can discriminate between fragments of mutant and wild type mtDNA. This was rather surprising, because the melting temperature predictions for hybrids between recombinant RNAs and mutated or wild type mtDNA (Table 1) show T_m values >37 °C. Thus, all RNA molecules tested are likely to anneal to mutant and wild type mtDNA fragments in the permissive conditions applied. According to the T_m predictions, we have started our experiments with shorter insertions of 8–10 nucleotides, which should anneal to mutant but not to wild type mtDNA. Surprisingly, we were not able to detect any signal with these RNA molecules used as probes for Southern blot hybridization and no effect on heteroplasmy level in transfected cells (data not shown). Then, we gradually increased the length of the complementary part from 11 to 25 nt and obtained specific hybridization (Fig. 2) for molecules containing 16- and 20-nt insertions. We suppose that the discrepancy between predictions and experimental data is due to the absence of software adapted to calculate the T_m of RNA-DNA duplexes containing a mismatch. Another possible explanation consists in formation of alternative secondary structures in RNA molecules that cannot be predicted by available software.

Another interesting issue is that the hybridization of RNA containing an insertion of the same length corresponding to the complementary L-strand of mtDNA (FD20L) was much less selective. This discrepancy can be explained by base mismatches: for FD20H, C-A pairing decreases the T_m of hybridization with wild type mtDNA by 10 °C (Table 1) compared with mutant mtDNA (predicted by IDT Sci-Tools OligoAnalyser software (version 3.1) for mismatch containing hybrids). In contrast, for FD20L, G-T pairing decreases T_m by only 5.5 °C and allows annealing of FD20L RNA with both mtDNA fragments at 37 °C. The above data show that a point mutation can be selectively addressed by RNA containing a 20-nucleotide stretch; however, for transitions A to G (in L-strand of mtDNA), sequences corresponding to H-strand would have a more selective effect and vice versa, for G to A transitions, only L-strand sequences should be used.

Pathogenic Mutation in ND5 Gene—mtDNA mutation A13514G, which we used as a model in the present study, is localized in NADH dehydrogenase ND5 subunit of the respiratory complex I. This is the first and largest enzyme of the respiratory chain (45 subunits, total size ~ 1 MDa), coupling electron transfer between NADH and ubiquinone to the translocation of four protons across the inner mitochondrial membrane (32). The L-shaped complex consists of hydrophilic and membrane domains. Three largest transmembrane subunits ND2, -4, and -5 at the far end of the membrane arm are homologous to each other and likely participate in the conformation-coupled proton translocation (33). Mutation A13514G induces amino acid replacement D393G localized in a very conserved region of ND5 transmembrane helix 12 (34, 35), forming the second half of the proton channel, and is involved in a cascade of conformational changes leading to proton translocation. Therefore, any mutation exchanging the negatively charged Asp-393 to uncharged amino acid residue could disturb the transport of the proton through the ND5 subunit channel of respiratory complex I.

The *ND5* gene turned out to be mutated frequently (30). Point mutation A13514G-inducing amino acid replacement D393G has been detected in four unrelated patients with MELAS-like and Leigh syndromes (19, 36, 37). Another transition, the frequently reported and well documented G13513A, affects the same Asp-393 residue in the *ND5* gene, but the amino acid replacement is different, D393N (reviewed in Ref. 30). A prominent clinical feature detected in patients with these mutations was a visual loss due to optic atrophy, indicating an exquisite sensitivity of the optic nerve to damage caused by alteration of the ND5 Asp-393 residue (38). Thus, search for Asp-393 mutations has been proposed to be a part of the routine screening for mitochondrial disorders (19).

More recently, among the patients with Leigh-like syndrome and D393N mutation in *ND5*, several cases were reported characterized by normal complex I activity in muscle (36, 39). The authors suggested that the relatively low mutant heteroplasmy and normal respiratory chain activities in muscle do not necessarily represent the situation in affected tissue such as brain and/or optic nerve. Thus, even low mutation load in Asp-393 in the presence of normal respiratory chain analysis may be considered as pathogenic (36), illustrating the complexities of correlating A13514G heteroplasmy levels with biochemical phenotype in patient's muscle and fibroblasts. This can be a characteristic feature of NADH dehydrogenase complex because it was recently demonstrated that even a low dose of wild type *ND6* gene is sufficient to drive assembly of near normal levels of complex I (6). All of these data taken together indicate that a low load of mutation A13514G might cause a functional defect of ND5 protein, but this defect would be very low and hardly noticeable. This is exactly the case of cells used in the present study.

Effect of Imported RNAs on mtDNA Heteroplasmy—As we have shown previously, mitochondrially imported anti-replicative RNAs can cause a replication stalling at the site of RNA annealing to the mutant mtDNA because of slowdown of the

replication fork progression (15). Nevertheless, we obtained only a transient shift of heteroplasmy in cells bearing a large deletion in mtDNA, the initial heteroplasmy level being restored in 6–8 days after cell transfection with anti-replicative RNA. This can be explained by recombinant RNA degradation, followed by preferential replication of shorter mitochondrial genomes bearing deletion, due to the previously reported effect of "replicative advantage of deleted mtDNA" (40). In the present study, we successfully obtained a stable decrease of the proportion of mtDNA molecules containing *ND5* point mutation after transfection of cybrid cells and primary fibroblasts with anti-replicative RNA FD20H (Fig. 5). Because no difference was expected in the rate of replication for wild type and mutant mtDNA, we can suggest that even after degradation of recombinant RNA, the induced shift in *ND5* point mutation heteroplasmy level may become stable. The maintenance of wild type mtDNA enrichment was previously reported for several mutations (41, 42).

Among several anti-replicative recombinant molecules, characterized by comparable stability in cells and mitochondrial import efficiency (Fig. 4), only FD20H was able to induce a prominent heteroplasmy shift. This RNA molecule demonstrated the highest ability to discriminate between mutant and wild type mtDNA (Fig. 2). The chimeric molecule, containing the same sequence of the insertion part as FD20H, but in the form of DNA, was not capable to shift the heteroplasmy level (Fig. 5). These data provide an additional proof of recombinant RNA action at the level of mtDNA replication because it was suggested that mitochondrial replisome helicase can separate DNA-DNA hybrids but not regions of short RNA-DNA hybrids in the mtDNA D-loop (43). Thus, only mitochondrially imported RNA (but not DNA) molecules are likely to function as anti-replicative agents in human mitochondria.

Cybrid cells used in the present study, containing 35% of mtDNA molecules bearing the A13514G mutation, were almost asymptomatic, characterized by a very slight decrease of all of the measurable parameters as oxygen consumption, levels of ATP, reactive oxygen species, and complex I enzymatic activity compared with wild type 143B cell line (data not shown). Nevertheless, we observed a prominent decrease of amount of mitochondria in cybrid cells, measured by use of MitoTracker Green, a mitochondria-selective fluorescent label, accumulating in the matrix (Fig. 5*C*) (44). Notably, transfection with anti-replicative RNA FD20H, leading to an important decrease of the level of *ND5* point mutation, caused, at the same time, a recovery of mitochondrial content. Unexpectedly, if the MitoTracker Green fluorescence increased gradually from day 4 to day 6 post transfection and then reached a plateau, the shift of the TMRM fluorescence between days 4 and 5 was rather sharp. Thus, we observe some temporary hyperpolarization of mitochondria only at day 5 post transfection. We can hypothesize that following the heteroplasmy decrease observed for *ND5* cybrid cells in 3–4 days post transfection, the synthesis of increased amounts of normal, fully active ND5 protein might create a temporary unbalance in the assembly of respiratory complexes, resulting in a rise of the basal production of reactive oxygen species (at the 5th day) and increasing mitochondrial biogenesis (days 6–8).

All of our data indicate on the possibility to obtain a curative effect of mitochondrial dysfunctions in human cells by a heteroplasmy shift induced by short RNA molecules targeted into mitochondria. Although the inhibitory effect was partial, it may have a long term therapeutic interest because only high levels of mutations in human mtDNA become pathogenic. The validation of the anti-replicative RNA strategy for a point mutation in mtDNA in cultured human cells can be considered as an important step to further develop an efficient therapy of mitochondrial diseases.

Acknowledgments—We are grateful to Massimo Zeviani (National Neurological Institute "Carlo Besta" of Milan) for providing the transmitochondrial cybrid cell lines and to Jérôme Mutterer (Institute of Molecular Biology of Plants, Strasbourg) for helpful assistance in confocal microscopy analysis. We also thank Virginie Girault, Catherine Murfitt, Laure Poirier, and Charlotte Simonin for experimental contributions.

REFERENCES

1. Burnett, J. C., and Rossi, J. J. (2012) RNA-based therapeutics: current progress and future prospects. *Chem. Biol.* **19,** 60–71
2. Ruiz-Pesini, E., Lott, M. T., Procaccio, V., Poole, J. C., Brandon, M. C., Mishmar, D., Yi, C., Kreuziger, J., Baldi, P., and Wallace, D. C. (2007) An enhanced MITOMAP with a global mtDNA mutational phylogeny. *Nucleic Acids Res.* **35,** D823–828
3. Wallace, D. C. (2010) Mitochondrial DNA mutations in disease and aging. *Environ. Mol. Mutagen.* **51,** 440–450
4. Rustin, P., H, T. J., Dietrich, A., R, N. L., Tarassov, I., and Corral-Debrinski, M. (2007) Targeting allotopic material to the mitochondrial compartment: new tools for better understanding mitochondrial physiology and prospect for therapy. *Med. Sci.* **23,** 519–525
5. Manfredi, G., Fu, J., Ojaimi, J., Sadlock, J. E., Kwong, J. Q., Guy, J., and Schon, E. A. (2002) Rescue of a deficiency in ATP synthesis by transfer of MTATP6, a mitochondrial DNA-encoded gene, to the nucleus. *Nat. Genet.* **30,** 394–399
6. Perales-Clemente, E., Fernández-Silva, P., Acín-Pérez, R., Pérez-Martos, A., and Enríquez, J. A. (2011) Allotopic expression of mitochondrial-encoded genes in mammals: achieved goal, undemonstrated mechanism or impossible task? *Nucleic Acids Res.* **39,** 225–234
7. Schneider, A. (2011) Mitochondrial tRNA import and its consequences for mitochondrial translation. *Annu. Rev. Biochem.* **80,** 1033–1053
8. Karicheva, O. Z., Kolesnikova, O. A., Schirtz, T., Vysokikh, M. Y., Mager-Heckel, A. M., Lombès, A., Boucheham, A., Krasheninnikov, I. A., Martin, R. P., Entelis, N., and Tarassov, I. (2011) Correction of the consequences of mitochondrial 3243A→G mutation in the MT-TL1 gene causing the MELAS syndrome by tRNA import into mitochondria. *Nucleic Acids Res.* **39,** 8173–8186
9. Kolesnikova, O. A., Entelis, N. S., Jacquin-Becker, C., Goltzene, F., Chrzanowska-Lightowlers, Z. M., Lightowlers, R. N., Martin, R. P., and Tarassov, I. (2004) Nuclear DNA-encoded tRNAs targeted into mitochondria can rescue a mitochondrial DNA mutation associated with the MERRF syndrome in cultured human cells. *Hum. Mol. Genet.* **13,** 2519–2534
10. Bacman, S. R., Williams, S. L., Garcia, S., and Moraes, C. T. (2010) Organ-specific shifts in mtDNA heteroplasmy following systemic delivery of a mitochondria-targeted restriction endonuclease. *Gene. Ther.* **17,** 713–720
11. Bacman, S. R., Williams, S. L., Hernandez, D., and Moraes, C. T. (2007) Modulating mtDNA heteroplasmy by mitochondria-targeted restriction endonucleases in a 'differential multiple cleavage-site' model. *Gene Ther.* **14,** 1309–1318
12. Taylor, R. W., Chinnery, P. F., Turnbull, D. M., and Lightowlers, R. N. (1997) Selective inhibition of mutant human mitochondrial DNA replication *in vitro* by peptide nucleic acids. *Nat. Genet.* **15,** 212–215

13. Muratovska, A., Lightowlers, R. N., Taylor, R. W., Turnbull, D. M., Smith, R. A., Wilce, J. A., Martin, S. W., and Murphy, M. P. (2001) Targeting peptide nucleic acid (PNA) oligomers to mitochondria within cells by conjugation to lipophilic cations: implications for mitochondrial DNA replication, expression and disease. *Nucleic Acids Res.* **29,** 1852–1863
14. Kolesnikova, O., Kazakova, H., Comte, C., Steinberg, S., Kamenski, P., Martin, R. P., Tarassov, I., and Entelis, N. (2010) Selection of RNA aptamers imported into yeast and human mitochondria. *RNA* **16,** 926–941
15. Comte, C., Tonin, Y., Heckel-Mager, A. M., Boucheham, A., Smirnov, A., Auré, K., Lombès, A., Martin, R. P., Entelis, N., and Tarassov, I. (2013) Mitochondrial targeting of recombinant RNAs modulates the level of a heteroplasmic mutation in human mitochondrial DNA associated with Kearns Sayre Syndrome. *Nucleic Acids Res.* **41,** 418–433
16. Zuker, M. (2003) Mfold web server for nucleic acid folding and hybridization prediction. *Nucleic Acids Res.* **31,** 3406–3415
17. Sugimoto, N., Nakano, S., Katoh, M., Matsumura, A., Nakamuta, H., Ohmichi, T., Yoneyama, M., and Sasaki, M. (1995) Thermodynamic parameters to predict stability of RNA/DNA hybrid duplexes. *Biochemistry* **34,** 11211–11216
18. Bellon, L. (2001) Oligoribonucleotides with 2′-*O*-(*tert*-butyldimethylsilyl) groups. in *Current Protocols in Nucleic Acid Chemistry*, pp. 1:3.6.1–3.6.13, John Wiley & Sons, Inc., New York
19. Corona, P., Antozzi, C., Carrara, F., D'Incerti, L., Lamantea, E., Tiranti, V., and Zeviani, M. (2001) A novel mtDNA mutation in the ND5 subunit of complex I in two MELAS patients. *Ann. Neurol.* **49,** 106–110
20. Smirnov, A. V., Entelis, N. S., Krasheninnikov, I. A., Martin, R., and Tarassov, I. A. (2008) Specific features of 5S rRNA structure: its interactions with macromolecules and possible functions. *Biochemistry* **73,** 1418–1437
21. Köhrer, C., Xie, L., Kellerer, S., Varshney, U., and RajBhandary, U. L. (2001) Import of amber and ochre suppressor tRNAs into mammalian cells: a general approach to site-specific insertion of amino acid analogues into proteins. *Proc. Natl. Acad. Sci. U.S.A.* **98,** 14310–14315
22. Smirnov, A., Tarassov, I., Mager-Heckel, A. M., Letzelter, M., Martin, R. P., Krasheninnikov, I. A., and Entelis, N. (2008) Two distinct structural elements of 5S rRNA are needed for its import into human mitochondria. *RNA* **14,** 749–759
23. Mager-Heckel, A. M., Entelis, N., Brandina, I., Kamenski, P., Krasheninnikov, I. A., Martin, R. P., and Tarassov, I. (2007) The analysis of tRNA import into mammalian mitochondria. *Methods Mol. Biol.* **372,** 235–253
24. Schneider, C. A., Rasband, W. S., and Eliceiri, K. W. (2012) NIH Image to ImageJ: 25 years of image analysis. *Nat. Methods* **9,** 671–675
25. Bolte, S., and Cordelières, F. P. (2006) A guided tour into subcellular colocalization analysis in light microscopy. *J. Microsc.* **224,** 213–232
26. Zinchuk, V., Zinchuk, O., and Okada, T. (2007) Quantitative colocalization analysis of multicolor confocal immunofluorescence microscopy images: pushing pixels to explore biological phenomena. *Acta Histochem. Cytochem.* **40,** 101–111
27. Zinchuk, V., and Grossenbacher-Zinchuk, O. (2009) Recent advances in quantitative colocalization analysis: focus on neuroscience. *Prog. Histochem. Cytochem.* **44,** 125–172
28. Gowher, A., Smirnov, A., Tarassov, I., and Entelis, N. (2013) Induced tRNA import into human mitochondria: implication of a host aminoacyl-tRNA-synthetase. *PLoS One* **8,** e66228
29. Tonin, Y., Heckel, A. M., Dovydenko, I., Meschaninova, M., Comte, C., Venyaminova, A., Pyshnyi, D., Tarassov, I., and Entelis, N. (2014) Characterization of chemically modified oligonucleotides targeting a pathogenic mutation in human mitochondrial DNA. *Biochimie* **100,** 192–199
30. Blok, M. J., Spruijt, L., de Coo, I. F., Schoonderwoerd, K., Hendrickx, A., and Smeets, H. J. (2007) Mutations in the ND5 subunit of complex I of the mitochondrial DNA are a frequent cause of oxidative phosphorylation disease. *J. Med. Genet.* **44,** e74
31. Davidson, S. M., Yellon, D., and Duchen, M. R. (2007) Assessing mitochondrial potential, calcium, and redox state in isolated mammalian cells using confocal microscopy. *Methods Mol. Biol.* **372,** 421–430
32. Efremov, R. G., and Sazanov, L. A. (2012) The coupling mechanism of respiratory complex I: a structural and evolutionary perspective. *Biochim. Biophys. Acta* **1817,** 1785–1795
33. Ohnishi, T., Ohnishi, S. T., Shinzawa-Itoh, K., Yoshikawa, S., and Weber, R. T. (2012) EPR detection of two protein-associated ubiquinone components (SQ(Nf) and SQ(Ns)) in the membrane *in situ* and in proteoliposomes of isolated bovine heart complex I. *Biochim. Biophys. Acta* **1817,** 1803–1809
34. Baradaran, R., Berrisford, J. M., Minhas, G. S., and Sazanov, L. A. (2013) Crystal structure of the entire respiratory complex I. *Nature* **494,** 443–448
35. Efremov, R. G., and Sazanov, L. A. (2011) Structure of the membrane domain of respiratory complex I. *Nature* **476,** 414–420
36. Brautbar, A., Wang, J., Abdenur, J. E., Chang, R. C., Thomas, J. A., Grebe, T. A., Lim, C., Weng, S. W., Graham, B. H., and Wong, L. J. (2008) The mitochondrial 13513G→A mutation is associated with Leigh disease phenotypes independent of complex I deficiency in muscle. *Mol. Genet. Metab.* **94,** 485–490
37. Bugiani, M., Invernizzi, F., Alberio, S., Briem, E., Lamantea, E., Carrara, F., Moroni, I., Farina, L., Spada, M., Donati, M. A., Uziel, G., and Zeviani, M. (2004) Clinical and molecular findings in children with complex I deficiency. *Biochim. Biophys. Acta* **1659,** 136–147
38. Chol, M., Lebon, S., Bénit, P., Chretien, D., de Lonlay, P., Goldenberg, A., Odent, S., Hertz-Pannier, L., Vincent-Delorme, C., Cormier-Daire, V., Rustin, P., Rötig, A., and Munnich, A. (2003) The mitochondrial DNA G13513A MELAS mutation in the NADH dehydrogenase 5 gene is a frequent cause of Leigh-like syndrome with isolated complex I deficiency. *J. Med. Genet.* **40,** 188–191
39. Sudo, A., Honzawa, S., Nonaka, I., and Goto, Y. (2004) Leigh syndrome caused by mitochondrial DNA G13513A mutation: frequency and clinical features in Japan. *J. Hum. Genet.* **49,** 92–96
40. Diaz, F., Bayona-Bafaluy, M. P., Rana, M., Mora, M., Hao, H., and Moraes, C. T. (2002) Human mitochondrial DNA with large deletions repopulates organelles faster than full-length genomes under relaxed copy number control. *Nucleic Acids Res.* **30,** 4626–4633
41. Bayona-Bafaluy, M. P., Blits, B., Battersby, B. J., Shoubridge, E. A., and Moraes, C. T. (2005) Rapid directional shift of mitochondrial DNA heteroplasmy in animal tissues by a mitochondrially targeted restriction endonuclease. *Proc. Natl. Acad. Sci. U.S.A.* **102,** 14392–14397
42. Suen, D. F., Narendra, D. P., Tanaka, A., Manfredi, G., and Youle, R. J. (2010) Parkin overexpression selects against a deleterious mtDNA mutation in heteroplasmic cybrid cells. *Proc. Natl. Acad. Sci. U.S.A.* **107,** 11835–11840
43. Bowmaker, M., Yang, M. Y., Yasukawa, T., Reyes, A., Jacobs, H. T., Huberman, J. A., and Holt, I. J. (2003) Mammalian mitochondrial DNA replicates bidirectionally from an initiation zone. *J. Biol. Chem.* **278,** 50961–50969
44. Presley, A. D., Fuller, K. M., and Arriaga, E. A. (2003) MitoTracker Green labeling of mitochondrial proteins and their subsequent analysis by capillary electrophoresis with laser-induced fluorescence detection. *J. Chromatogr. B. Analyt. Technol. Biomed. Life Sci.* **793,** 141–150

Modeling of Antigenomic Therapy of Mitochondrial Diseases by Mitochondrially Addressed RNA Targeting a Pathogenic Point Mutation in Mitochondrial DNA

Yann Tonin, Anne-Marie Heckel, Mikhail Vysokikh, Ilya Dovydenko, Mariya Meschaninova, Agnès Rötig, Arnold Munnich, Alya Venyaminova, Ivan Tarassov and Nina Entelis

J. Biol. Chem. 2014, 289:13323-13334.
doi: 10.1074/jbc.M113.528968 originally published online April 1, 2014